(26) Jeener, J.; Broekaert, P. *Phys. Rev.* **1967**, *157*, 232.
(27) Van Geet, A. L. *Anal. Chem.* **1970**, *42*, 679.
(28) Mehring, M. *NMR: Basic Principles and Progress*; Springer-Verlag: Berlin, 1976; Vol. 11, Chapter V.
(29) Bertrand, R. D.; Moniz, W. B.; Garroway, A. N.; Chingas, G. C. *J. Am. Chem. Soc.* **1978**, *100*, 5227.
(30) Chingas, G. C.; Garroway, A. N.; Bertrand, R. D.; Moniz, W. B. *J. Chem. Phys.* **1981**, *74*, 127.
(31) VanderHart, D. L.; Earl, W. L.; Garroway, A. N. *J. Magn. Reson.* **1981**, *44*, 361.
(32) Odajima, A.; Sauer, J. A.; Woodward, A. E. *J. Polym. Sci.* **1962**, *57*, 107.
(33) Willenberg, B.; Sillescu, H. *Makromol. Chem.* **1977**, *178*, 2401.
(34) Lindner, P.; Rossler, E.; Sillescu, H. *Makromol. Chem.* **1981**, *182*, 3653.
(35) Spiess, H. W. *Colloid Polym. Sci.* **1983**, *261*, 193.
(36) Bergmann, K. *Kolloid Z. Polym.* **1973**, *251*, 962.
(37) Olf, H. G.; Peterlin, A. *Kolloid Z. Z. Polym.* **1967**, *215*, 97.
(38) Guenet, J. M.; McKenna, G. B. *Macromolecules*, in press.
(39) Goldman, M. *Spin Temperature and Nuclear Magnetic Resonance in Solids*; Oxford University Press: London, 1970; Chapter 3.
(40) Yang, Y. C.; Geil, P. H. *J. Macromol. Sci.* **1983**, *B22*(3), 463.
(41) Painter, P. C.; Kessler, R. E.; Snyder, R. W. *J. Polym. Sci., Polym. Phys. Ed.* **1980**, *18*, 723.
(42) Swalin, R. A. *Thermodynamics of Solids*; Wiley: New York, 1972, p 180 ff.
(43) Abragam, A. *Principles of Nuclear Magnetism*; Oxford University Press: London, 1961; Chapter V.
(44) Packer, K. J.; Pope, J. M.; Yeung, R. R.; Cudby, M. E. A. *J. Polym. Sci., Polym. Phys. Ed.* **1984**, *22*, 589.
(45) Randall, J. C. *J. Polym. Sci., Polym. Phys. Ed.* **1975**, *13*, 889.
(46) Earl, W. L.; VanderHart, D. L. *J. Magn. Reson.* **1982**, *48*, 35.
(47) *Atlas of Carbon-13 NMR Data*; Breitmaier, E., Haas, G., Voelter, W., Eds.; Heyden: London, 1979.
(48) VanderHart, D. L. *J. Chem. Phys.* **1986**, *84*, 1196.
(49) Cohen-Addad, J. P. In *Structure and Dynamics of Molecular Systems-II*; Daudel, R., Ed.; Reidel: Dordrecht, Holland, 1986; p 155 ff.
(50) Cahn, J. W. *J. Am. Ceram. Soc.* **1969**, *52*, 118.

Microdomain Characterization of Styrene–Imidazole Copolymers

R. C. Sutton, L. Thai, J. M. Hewitt, C. L. Voycheck, and J. S. Tan*

Research Laboratories, Eastman Kodak Company, Rochester, New York 14650. *Received August 21, 1987*

ABSTRACT: The microstructures of several copolymers of styrene and *N*-vinylimidazole in dilute solutions and cast films were investigated by fluorescence, ^{13}C NMR, light scattering, viscosity, and electron microscopy. Random sequence distribution of the copolymers was characterized by ^{13}C NMR. Despite such random distribution of the styrene and imidazole groups along the chain, phase separation of the hydrophobic styrene and the hydrophilic imidazole domains is suggested by several experimental findings. Smaller hydrodynamic volumes of such styrene–imidazole copolymers in polar solvents were measured compared to those for the homopolymer, poly(*N*-vinylimidazole), at comparable molecular weights. This is attributed to the aggregation of styrene residues in the polar environment. A sharp conformational change of these copolymers in aqueous media from a supercoiled dispersion to a water-soluble extended coil can be induced by protonation of the imidazole moiety. Local aggregation of the styrene groups and electrostatic repulsion of the protonated imidazolium groups are the causes for such a transition. The styrene aggregation was further characterized by the styrene emission spectra of the copolymers. The excimer-to-monomer peak ratio of the intrinsic styrene chromophore varies with copolymer composition, solvent, and pH, suggesting the effect of long-range interaction on styrene excimer formation. Separation between the styrene and imidazole domains was further verified by the absence of energy transfer from the styrene chromophore as the donor to an acceptor probe, 1-pyrenesulfonic acid, complexed at the imidazole site. Such phase separation is manifested in films cast on water from organic solutions of the copolymers. These results suggest that the hydrophobic/hydrophilic random copolymers behave as polymeric surfactants characterized by a micellelike structure in an aqueous environment.

Introduction

For various applications of polymers, copolymers are frequently employed to achieve optimal functionalities of the component comonomers. Random copolymers of styrene and *N*-vinylimidazole as shown by the following formula are such examples.

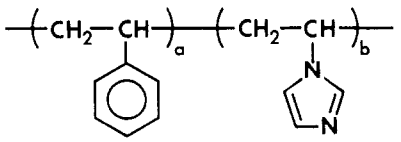

The hydrophilic imidazole moiety is used to provide the reactive sites for metal ion complexation, dye binding, or oxygen quenching; the hydrophobic styrene moiety is used to enhance the binding strength of dye molecules and other desired physical properties in the film. These properties are greatly affected by the microstructures of the copolymers in solutions and solid states. The objective of the present work is to characterize the microstructures of such systems by using various microscopic and macroscopic techniques. Correlation between polymer structures and interactions with dye molecules will be reported in a separate paper.[1]

While phase separation is a common phenomenon in block and graft copolymers, less is known about random copolymers. Because of the diametric solubility behavior of the component styrene and imidazole moieties, polymer conformation and the morphology of cast film can be manipulated by the nature of the solvent. In the present study, several experimental facts are provided to support the existence of styrene-phase formation.

In an aqueous medium, formation of a micellelike dispersion is expected, consisting of the water-insoluble styrene core and the water-soluble imidazole groups distributed on the surface of the dispersion. Such a process is driven by an entropic gain associated with the migration of the hydrophobic styrene groups from an aqueous environment to the interior of the polymer dispersion. The flexibility of the backbone chain is required for this segmental reorientation. Such micellelike structures can be altered by solvent or pH changes as depicted in Figure 1. In an acidic medium, the polymer coil is extended and soluble in water (structure a), resulting from protonation of the imidazole groups. An increase in pH above 4.0

0024-9297/88/2221-2432$01.50/0

Table I
Characterization Data for StIm Copolymers

polym	[St]/[Im]	$10^{-4}M_w$	[η] (MeOH/TBA-Br), dL/g	^{13}C NMR rel int of components of StIm imidazole CH peak: St–Im–St[a] (54.9 ppm)	Im–Im–St + St–Im–Im (53.9 ppm)	Im–Im–Im (52.4 ppm)	T_g,[b] °C
StIm-30	30/70	7.7		1.0 (1.0)	5.2 (4.8)	6.4 (5.7)	147 (144)[c]
StIm-47	47/53	8.3		1.0 (1.0)	2.8 (2.2)	2.3 (1.3)	145
StIm-56	56/44	6.7	0.198 (slightly hazy)	1.0 (1.0)	2.05 (1.6)	1.15 (0.6)	138
StIm-50	50/50	7.7	0.38				
		5.2	0.26				
		4.9	0.22				

[a] The imidazole CH peak intensity at St–Im–St was taken as unity. [b] The T_g data were measured by A. Marshall of these Laboratories. The T_g for PVI is 182 °C and for polystyrene is 100 °C. [c] This T_g was for the film sample cast on water.

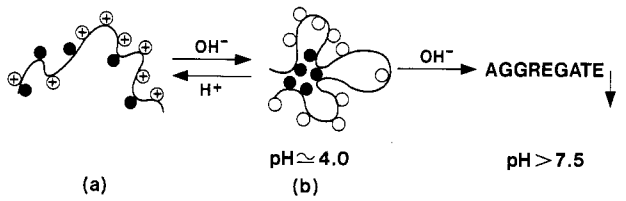

Figure 1. Conformational change of StIm copolymers in aqueous solution. (● represents styrene and ○ or ⊕ represent imidazole and imidazolium groups, respectively.)

facilitates the micelle formation as shown by structure b. Further increase in pH above 7.0 causes complete deprotonation of the imidazole group and the consequent precipitation of the polymer.

Several fluorescence probes are known to have high quantum yield in nonpolar media and to have their emission quenched in aqueous media. Such molecules have been used to probe conformational changes in proteins[2] and synthetic polyelectrolytes.[3-5] In this study, we have chosen pyrene and *N*-phenyl-1-naphthylamine as the probes. Conformational changes of the copolymers induced by pH as described in Figure 1 were monitored by changes in fluorescence intensities. An alternative method, the steady-state fluorescence polarization, also provides a sensitive tool to probe rotational mobility of the molecule. We have used 1-pyrenesulfonic acid to complex the copolymers at the imidazole site. Conformational changes induced by pH were followed by measuring the polarization of the probe. The conformational transition region observed by the above static and dynamic structural characterization of fluorescence will be compared.

The styrene-phase formation in the copolymers was examined by the emission spectra of the intrinsic styrene chromophore. The excimer-to-monomer peak ratio of the copolymer solution and film samples, as a function of copolymer composition, solvent, and pH, was used as a measure of the extent of styrene aggregation. Phase separation of the styrene and imidazole microdomains in aqueous solutions was further investigated by energy transfer. In this measurement, the intrinsic styrene chromophore was used as the donor and the extrinsic probe, 1-pyrenesulfonate complexed at the imidazole site, was used as the acceptor.

Phase separation in the aqueous dispersion observed by the above fluorescence techniques was compared to that of films cast on water from a 2-methoxyethanol solution of the copolymers and measured by transmission electron microscopy.

Experimental Section

Materials. The homopolymer, poly(*N*-vinylimidazole) (PVI), used in this study, was a fraction with a weight-average molecular weight of 150 000 prepared for a previous work.[6] The homopolymer, poly(styrene), was a sample with a molecular weight of 110 000 from Pressure Chemical Co.

The copolymers of styrene (St) and *N*-vinylimidazole (Im) were synthesized by a continuous, free-radical-initiated polymerization process as previously described.[7] The monomers, styrene (Dow Chemicals) and *N*-vinylimidazole (BASF Chemicals), were freshly distilled before polymerization. The initiator, azobis(isobutyronitrile) (AIBN, Kodal Laboratory Chemicals), was used without further purification.

The polymerization was conducted at 120 °C in two 2-L glass reactors connected in series and filled with the solvent *N*,*N*-dimethylformamide (DMF). A stream of 0.4 mL/min of a mixture of St and Im monomers at a given molar ratio and a stream of 0.4 mL/min of the AIBN (1% based on the weight of the monomers) dissolved in DMF were introduced simultaneously to the first reactor, all solutions being previously purged with N_2. A second stream of 0.2 mL/min of the AIBN in DMF (0.5% based on the weight of the monomers) was separately introduced to the second reactor to complete the reaction of the unreacted monomers from the first reactor. The overflow from the second reactor was discarded until a steady state was attained. The residence time of the mixture, as determined by the volume of reactor/total flow rate, was typically 5 h. The collected polymer solution was diluted with DMF and precipitated in the stirred distilled water. The solids were washed several times with water and dried in vacuo at 60 °C for 4 days. The compositions of the copolymers were analyzed by elemental analysis, GC, and potentiometric titration. The molar ratio of the feed monomers and the final copolymer were in good agreement. The compositions of several of the copolymers and their corresponding weight-average molecular weights are listed in Table I.

The reactivity ratios for the monomers, r_1 (styrene) and r_2 (imidazole), were calculated from the average composition of a series of copolymerizations by using the following equation

$$d[St]/d[Im] = \frac{[St](r_1[St] + [Im])}{[Im](r_2[Im] + [St])}$$

where [St] and [Im] are the concentrations of the monomers and d[St] and d[Im] are the corresponding rates of concentration change. The concentrations were determined by GC, elemental analysis, and potentiometric titration of the imidazole group. The reactivity ratios thus obtained are $r_1 = 8.1$ and $r_2 = 0.13$, comparable to those reported by Petrak[8] for the same copolymers but made by bulk polymerization.

The fluorescent dyes, pyrene (Py, Aldrich), *N*-phenyl-1-naphthylamine (NPN, Kodak Research Chemicals), and 1-pyrenesulfonic acid (Py-SO_3H, Molecular Probes), were used without further purification.

Methods. Light Scattering and Intrinsic Viscosity. The weight-average molecular weights $\bar{M}_w$ of the StIm copolymers were measured at 25 °C in MeOH/0.001 M tetrabutylammonium bromide (TBA-Br) with a C. N. Wood photometer equipped with unpolarized light at 436 nm. The intrinsic viscosity [η] data at 25 °C were obtained in an Ubbelöhde microviscometer. Details of such measurements are similar to those described elsewhere.[6,9]

Potentiometric Titration. The determination of the imidazole contents of the StIm copolymers was carried out in acetonitrile/MeOH (1/1, v/v) containing 1 M TBA-Br, similar to those

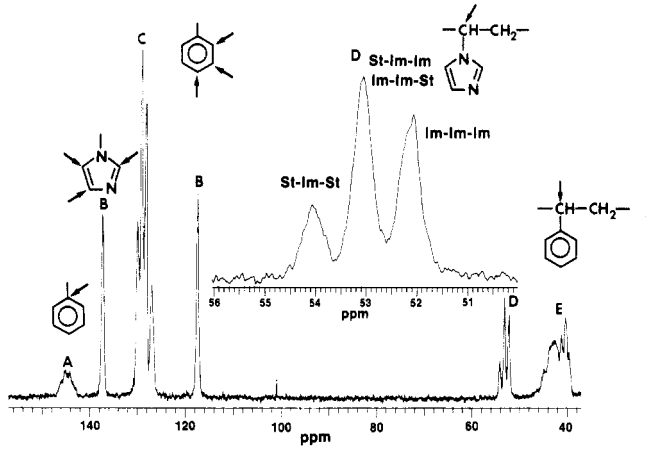

Figure 2. ^{13}C NMR spectra of StIm-47 in DMF-d_7. The peak assignments are made according to the spectra of the homopolymers, PVI and polystyrene, and are shown in the figure.

reported for the PVI homopolymer.[10] Sharp and single titration end points were obtained for all copolymers studied. The absence of two distinct inflections, a typical behavior for the PVI homopolymer resulting from nearest-neighbor H-bonding between the protonated and unprotonated imidazole groups,[10] suggests that there is no measurable amount of the PVI homopolymer in the final copolymer products after washing and precipitation from water. The absence of two inflections also yields some information about the monomer sequence in the copolymers. The titration curve for the partially quaternized PVI showed that 3–4 imidazole units are the minimum block length needed to observe two distinctive inflections. Such random sequencing of imidazole groups in the present copolymers is consistent with the T_g data and the ^{13}C NMR results discussed below.

^{13}C NMR Spectroscopy. ^{13}C NMR spectra were used to analyze the monomer distribution of the StIm copolymers. The spectra of the polymer solutions in DMF-d_7 were acquired at 75.4 MHz, using a Varian XL300A spectrometer at room temperature with 40 000 scans for each sample. A 1.5-s delay was used between 45 pulses. Precautions were taken in accumulating the spectra to ensure that saturation and NOE had small effects on the intensities of the CH backbone resonances. The peak assignments as shown in Figure 2 were made by comparing those of the homopolymers, poly(styrene) and PVI.

Sequence information for any polymer from ^{13}C data can be obtained from resonances whose chemical shifts are sensitive to changes in the environment resulting from sequence differences. The CH carbon resonance of imidazole is the only resonance from the copolymer which displays the sensitivity for such analysis. The backbone CH carbon resonance of the imidazole in the StIm copolymers consists of three components corresponding to the three nearest-neighbor monomer sequence environments, i.e., St–Im–St, Im–Im–St, and Im–Im–Im. Previous studies have shown that the CH resonance of the PVI homopolymer is only slightly affected by tacticity,[12] and hence we infer that the three resonances we observed here are caused by sequencing effect only. The relative intensities of these peaks were used to calculate the sequence distribution of the monomer units. The results for the three measured imidazole CH peak intensities are shown in Table I. Also listed in the parentheses are the corresponding calculated intensities according to Bernoulian random statistics[13] based on the fact that the product of the reactivity ratios of the two monomers is approximately unity, i.e., $r_1r_2 = 1.05$, as described earlier in the synthesis. The approximate agreement of the measured and calculated values indicates that these copolymers appear to be much closer to having a random sequence distribution rather than being blocked.

The single T_g values for these materials, also listed in Table I, support this conclusion. The T_g values for the copolymers are approximately equal to those estimated from the mole-fraction-weighted averages from the corresponding values for the homopolymers, poly(styrene) and PVI.

Fluorescence Spectroscopy. The emission spectra were recorded at room temperature on the SLM-4800 spectrofluorometer. All spectra were corrected with a glycerol solution of Rhodamine B as the reference quantum counter. The styrene emission spectra of the copolymer solutions excited at 260 nm were collected in a 3 mm × 3 mm quartz cell to avoid inner cell quenching. For the film samples, the front-surface illumination using a 253.3-nm filter for the excitation source was applied to avoid scattering and light leaks from the monochromator. Each styrene spectrum was acquired with 10 multiple scans. Care was taken to avoid any significant solvent emission, and subtraction of the solvent spectra was applied to all styrene emission data.

The emission spectra of the pyrene and *N*-phenyl-1-naphthylamine (NPN) in the aqueous dispersion of the StIm copolymers were obtained by exciting at 340 nm. The peak intensities at 374 nm for pyrene and 420 nm for NPN were used to monitor conformational change as a function of pH. Since the transition region was found to be independent of the presence of dissolved oxygen in the solution, all solutions were not purged with N_2 before measurements.

Steady-state fluorescence polarization was also measured on the SLM-4800 instrument equipped with two polarizers at the excitation and emission slits. The polarization was calculated according to $p = (R - 1)/(R + 1)$ where

$$R = (I_{vv}/I_{vh})/(I_{hv}/I_{hh})$$

The subscripts for the intensities I's in the above equation refer to the vertically (v) and horizontally (h) polarized light. The first subscript is for the excitation and the second is for the emission. The denominator in the expression for R is the grating correction factor.

The solutions of the copolymers complexed with the dye, 1-pyrenesulfonic acid (Py-SO_3H), were excited at 350 nm and the data for P were collected at 385 nm.

Turbidimetric Titration. The turbidity of the aqueous copolymer solution as a function of pH at 25 °C was measured by the optical density at 450 nm by using a Varian Superscan-3 spectrophotometer.

Transmission Electron Microscopy. The thin films were prepared by casting from solution. A few drops of the StIm-30 stock solution in 2-methoxyethanol (2.74%) were placed on distilled water. The thin films (0.1 μm) were picked off the surface of the water directly onto a 200-mesh copper grid. The samples were air dried and then examined by transmission electron microscopy (TEM). Electron micrographs were obtained with a JEOL 100S electron microscope operated at 80 kV.

The transmission electron micrographs were also obtained for the aqueous dispersion of the copolymers. A few microliters of the above StIm-30 stock solution were dispersed into 3 mL of vigorously stirred distilled water. Formvar and carbon-coated copper grids were treated with the above dispersion. After 30 s, excess liquid was wicked away with the edge of a filter paper and the grid allowed to air dry before taking the TEM.

Results and Discussion

Hydrodynamic Volume in MeOH/0.001 M TBA-Br. The intrinsic viscosity data for the three molecular weight samples of StIm-50, as listed in Table I, were measured by G. Russell, formerly of these Laboratories. They are plotted against $\bar{M}_w$ in Figure 3. Also included for comparison are the data for poly(*N*-vinylimidazole) reported previously.[6] The Mark–Houwink exponent for PVI was 0.67, indicating that MeOH is a reasonably good solvent for the homopolymer. This is attributed to the hydrogen bonding between the solvent OH group and the lone-paired electrons at the aromatic nitrogen site of the polymer.

The smaller values of $[\eta]$ for the present copolymers compared to that of PVI at a given $\bar{M}_w$, as shown in Figure 3, suggest that the hydrodynamic volume is reduced by incorporating the styrene comonomer. Aggregation of the styrene residue in MeOH, which is a nonsolvent for polystyrene, is clearly an explanation for this chain contraction. Such behavior becomes more pronounced when the styrene content increases. This is demonstrated by the lower value for StIm-56 as shown in Table I and Figure 3.

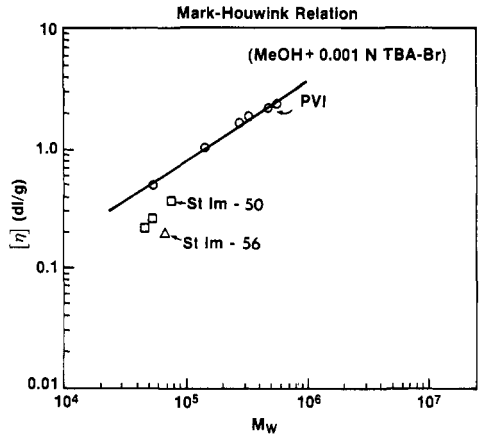

Figure 3. Mark–Houwink plot, $[\eta]$ versus $\bar{M}_w$ for PVI, StIm-50, and StIm-56 in MeOH/0.001 N TBA-Br.

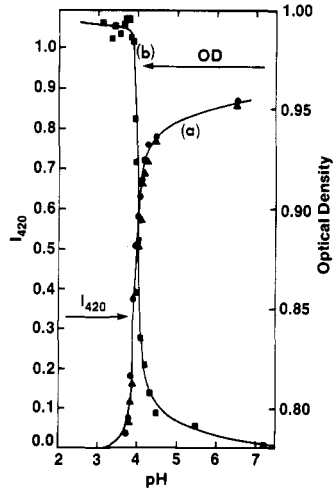

Figure 4. Relative fluorescence intensity I_{420} for NPN (2×10^{-5} M) in StIm-30 aqueous dispersion ([Im] = 2×10^{-4} M; [St] = 8.4×10^{-5} M) versus pH (a); optical density of StIm-30 aqueous dispersion versus pH (b).

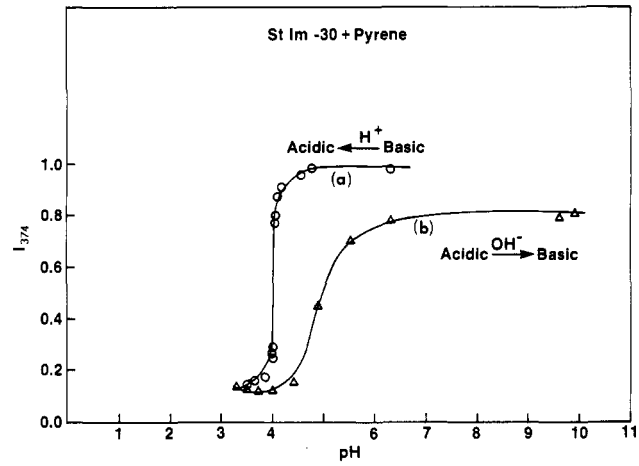

Figure 5. Relative fluorescence intensity I_{374} for pyrene in StIm-30 aqueous dispersion ([Im] = 2×10^{-4} M; [St] = 8.4×10^{-5} M) versus pH, from basic to acidic (a) and from acidic to basic (b).

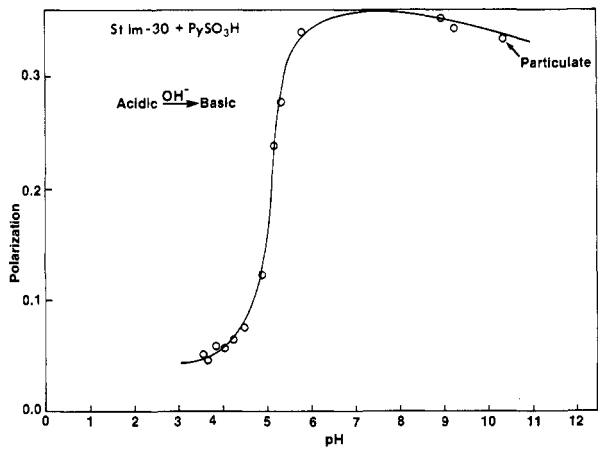

Figure 6. Steady-state fluorescence polarization P versus pH for Py-SO_3^- complexed with StIm-30 ([Im] = 2×10^{-4} M; [St] = 8.4×10^{-5} M).

Conformational Change in Aqueous Media. The aqueous dispersion of the copolymer was prepared by dispersing 3 μL of a 2-methoxyethanol stock solution of the copolymer into a 1 cm × 1 cm cuvette containing 3 mL of well-stirred deionized water. The dispersion ([Im] = 2×10^{-4} M; [St] = 8.4×10^{-5} M) consists of small intermolecular aggregates ranging from 1 to 0.1 μm as observed by TEM.

The fluorescence titration curve of such aqueous dispersion containing 2×10^{-5} M of the NPN dye is shown as curve a in Figure 4. In this experiment, microliter increments of 0.1 M HCl were added to 3-mL copolymer dispersions, and the peak intensities at 420 nm were recorded as a function of pH measured simultaneously with a pH microelectrode immersed in the cuvette. A sharp transition region at pH 4 is shown for StIm-30. This transition region also coincides with that observed by the turbidimetric titration shown as curve b in Figure 4. This transition is a result of conformational change of the copolymer from a supercoiled compact dispersion to a water-soluble extended coil upon protonation of the imidazole groups.

The above finding was also confirmed by a separate titration run using pyrene (2×10^{-6} M) as the probe. An identical sharp transition at pH 4 is also shown by curve a in Figure 5, where the relative fluorescence intensity of pyrene at 374 nm is plotted against pH for the same polymer dispersion. Also plotted in the same figure as curve b are the intensity data when an acidic solution of the polymer was titrated with 0.1 M NaOH. It is to be noted that a broader transition with the midpoint shifted to pH 5 was obtained when the titration was carried out from acidic to basic media. Such "hysteresis" effect is a useful phenomenon to be exploited for blending such copolymers with other water-soluble polymers in aqueous media.

A similar titration behavior of StIm-30 from acidic to basic media was observed through the steady-state fluorescence polarization data, as shown in Figure 6. In this experiment, an anionic probe, Py-SO_3H (5×10^{-7} M), was complexed at the imidazole site of the copolymer ([Im] = 2×10^{-4} M; [St] = 8.4×10^{-5} M). The polymer has undergone a conformational change from a flexible freely rotating chain at low pH, as reflected by the low polarization of 0.05, to a rigid compact coil at high pH with the polarization increased to 0.35 before precipitation.

Styrene Emission Spectra. There have been many studies on the styrene fluorescence behavior of neutral poly(styrene)[14-18] and some block[19] or random[20,21] styrene-containing copolymers in organic solvents. However, little has been explored using the styrene comonomer as an intrinsic probe for structural characterization in aqueous media. Several reports were recently published on sodium poly(styrenesulfonate) (NaPSS) in aqueous salt solutions. It is generally believed that excimer formation in such homopolymers is dominated by nearest-neighbor

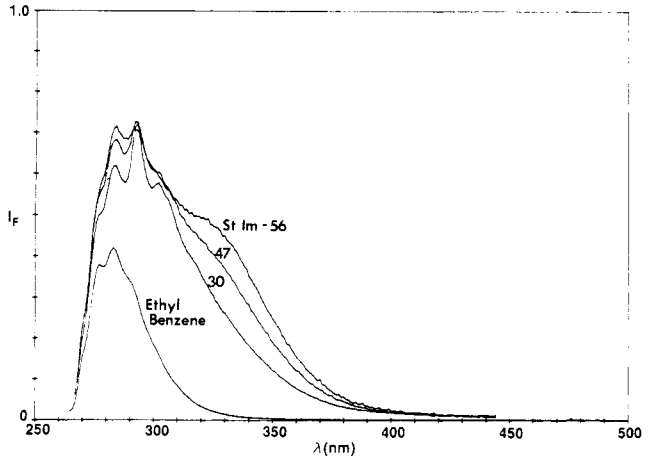

Figure 7. Emission spectra for StIm-30, -47, and -56 ([St] = 0.005 M) and ethyl benzene in MeOEt.

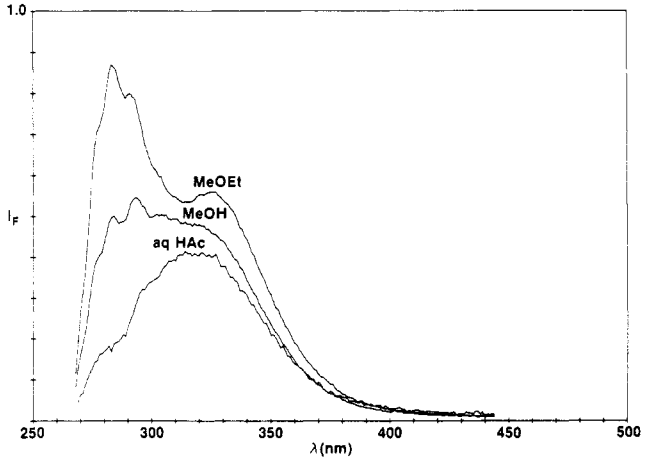

Figure 8. Emission spectra for StIm-56 ([St] = 0.0066 M) in MeOEt, MeOH, and aqueous acetic acid solutions.

interaction between pairs of fully eclipsed, sandwiched phenyl rings and largely by those located at the meso diads in the trans-trans conformation.[25] Long-range interactions caused by the effects of good solvents or counterions for polyelectrolytes play an insignificant role in determining such local behavior. While some evidence was reported that the excimer to monomer peak ratio, I_E/I_M, increases with ionic strength (>0.1 M) for NaPSS[24] and KPSS, CaPSS, SrPSS, and LaPSS,[23] long-range chain contraction has not been accounted for in such findings. Furthermore, long-range end-to-end chain cyclization between two pyrene end groups in poly(oxyethylene), where excimer formation is dependent on solvent, has been ruled out for the styrene chromophore because of its short lifetime. Our data presented below for the random styrene-containing copolymers provide some insight to the effect of long-range forces on local excimer formation.

Figure 7 shows the emission spectra of the three StIm copolymers at a comparable $\bar{M}_w$ (see Table I) in a good organic solvent, 2-methoxyethanol (MeOEt). Also shown for comparison is the spectrum for ethylbenzene. The peaks at 280, 285, and 293 nm are clearly attributed to the monomer peaks, and 330 nm is the excimer peak. The more obvious excimer shoulder for the StIm-56 compared with those for StIm-47 and -30 is a result of the higher content of styrene nearest-neighbor pairs in the former. Interchain styrene excimer formation is unlikely to occur in such low polymer concentration dilute solutions (approximately 0.1% of copolymers corresponding to [styrene] = 0.005 M in a good organic solvent).

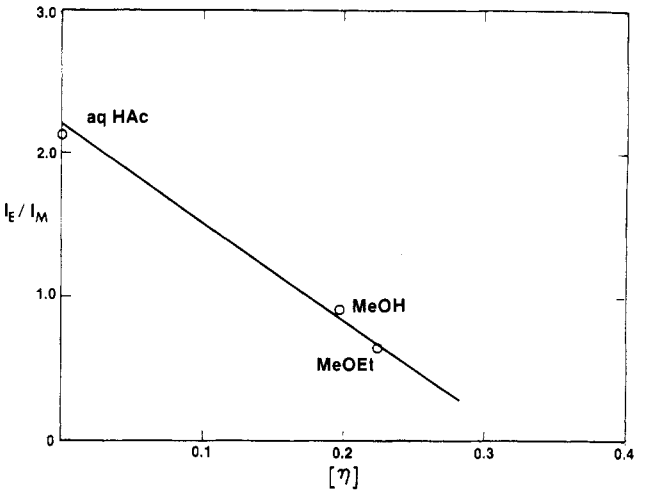

Figure 9. I_E/I_M (I_{330}/I_{285}) versus [η] for StIm-56 in MeOEt, MeOH, and aqueous acetic acid solutions (pH 3.0).

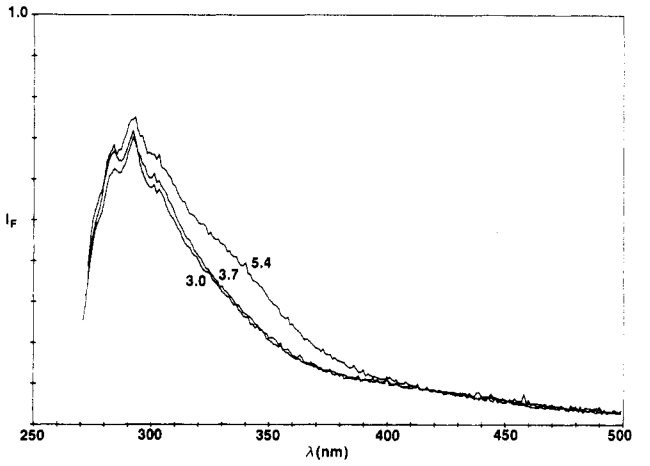

Figure 10. Emission spectra for StIm-30 ([St] = 0.005 M) in aqueous acetic solutions pH 3.0, 3.7, and 5.4.

The effect of solvent on the styrene emission of StIm-56 is shown in Figure 8. To avoid the possible effect of oxygen quenching on excimer formation, all samples were purged with N_2 before measurement. The shapes of the spectra remained unchanged. The extent of excimer formation as indicated by the I_E/I_M values in the three solvents (i.e., I_E/I_M = 0.64, 0.92, and 2.12 in MeOEt, MeOH, and aqueous HAc, respectively) is most pronounced in aqueous acetic acid solution and decreases in the good solvent MeOEt.

In order to examine the effect of long-range forces resulting from polymer segment–solvent interaction, the intrinsic viscosity measurements were made for the same StIm-56 copolymer in the three solvents shown in Figure 8. The relation between I_E/I_M and [η] is presented in Figure 9 The linear increase of the excimer formation with decreasing [η] clearly gives evidence for the effects of long-range forces or chain expansion on styrene–ring interaction. Similar arguments were also given by Frank et al.[26] for pyrene-labeled poly(ethylene glycol) based on solvent viscosity. The possibility for interchain aggregation in the aqueous acetic acid medium (pH 3.0) was ruled out because of low polymer concentration and also the copolymer was completely soluble when it was fully protonated.

The excimer formation resulting from intermolecular aggregation in aqueous dispersion is observable, however, if the pH is raised above the transition region (pH 5) as displayed in Figures 5 and 6. The emission spectra for StIm-30 in aqueous solutions as a function of pH are shown

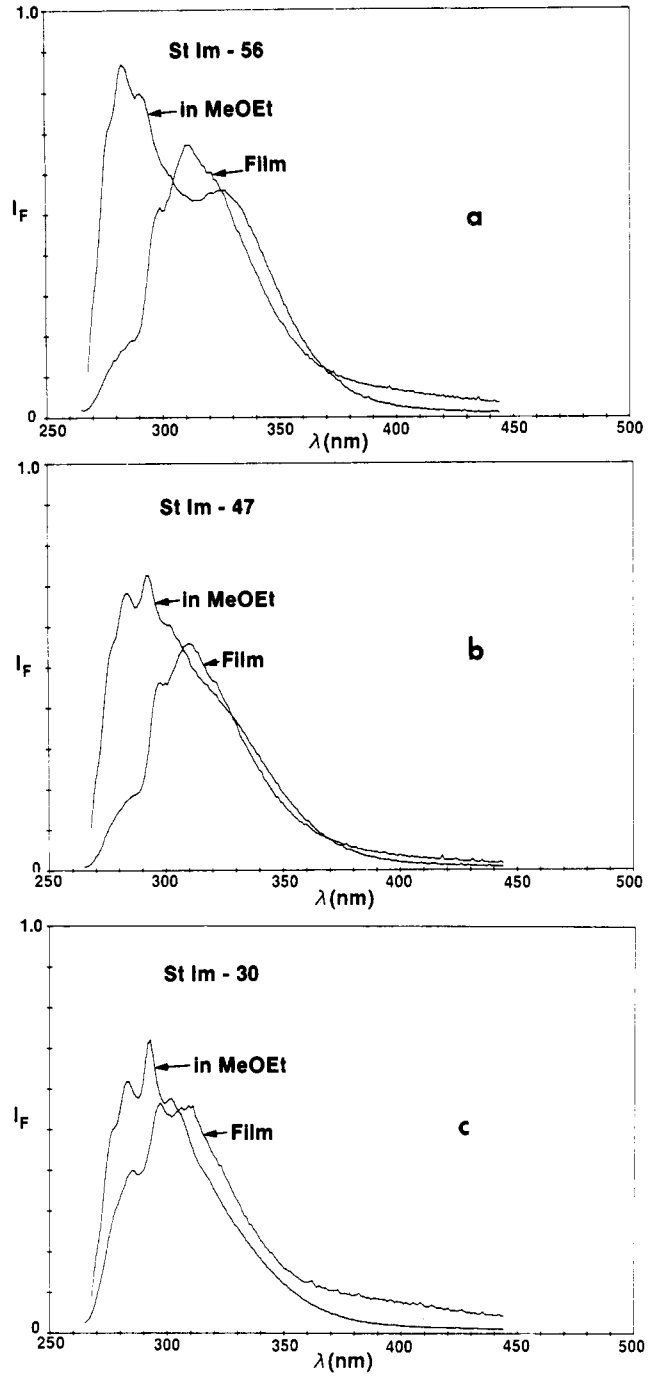

Figure 11. (a) Emission spectra of StIm-56 in films and in MeOEt. (b) Emission spectra of StIm-47 in films and in MeOEt. (c) Emission spectra of StIm-30 in films and in MeOEt.

in Figure 10. The increasing shoulder at the 330-nm excimer peak for the pH 5.4 sample demonstrates the effect of chain coiling by deprotonation, as well as some interchain aggregation, on excimer formation. Similar behavior was also reported by Webber et al.[27] for a random copolymer of 2-vinylnaphthalene and maleic acid in aqueous media.

Comparison of the emission spectra for the solution and film samples of the three copolymers are shown in Figure 11. The excimer peak, which is predominant in the films, was shifted to 310 nm. Isolation of the monomer and excimer peaks by a curve-resolving technique was not attempted because of the broad nature and peak shifting of the emission.

The above findings suggest that excimer formation in random copolymers is a result of styrene aggregation.

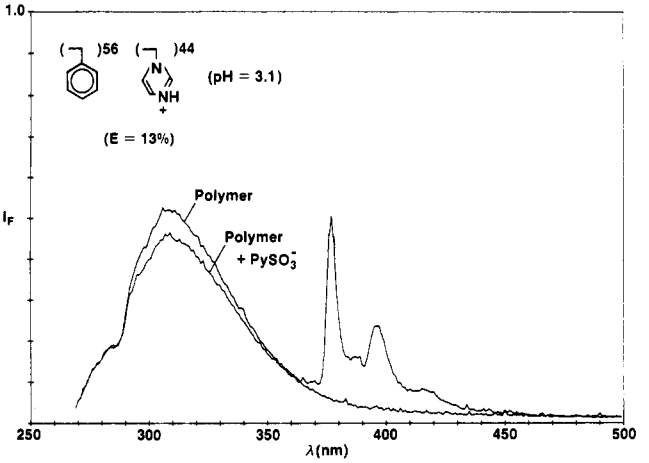

Figure 12. Emission spectra of StIm-56 ([St] = 0.005 M) in aqueous acetic acid (pH 3.1) in the absence and presence of the acceptor Py-SO_3^- (4×10^{-7} M).

While nearest-neighbor pairing of the phenyl groups is a prerequisite for such excimer formation, it is enhanced by the long-range intrachain and interchain interactions in solutions.

Phase Separation between Styrene and Imidazole Domains. Energy-transfer experiments were carried out to examine phase separation between the hydrophobic styrene domain in the core and the hydrophilic imidazole domain on the outer layer of the copolymer aqueous dispersion. The intrinsic styrene chromophore was used as the donor, which was excited at 260 nm and emitted as an excimer in the range from 300 to 350 nm. An extrinsic probe, 1-pyrenesulfonic acid (Py-SO_3^-) complexed at the imidazole site, was used as the acceptor. This probe was excited in the range of the styrene excimer emission and emitted at 375–420 nm. The concentration of the styrene in the copolymer solution was kept at 0.005 M and that of the $PySO_3^-$ probe was kept at 4×10^{-7} M. Complete binding of the probe was checked by spectrophotometric titrations to be discussed in a later paper.[1]

The emission spectra of styrene in the presence and absence of the acceptor are shown in Figure 12 for StIm-56 in an aqueous acetic acid medium at pH 3.1. Energy transfer is indicated by the decrease of the styrene emission in the presence of the acceptor. The energy transfer efficiency, $E = 13\%$, was estimated by the intensities at 315 nm and the following relation:

$$1 - E = I_{(\text{polymer})}/I_{(\text{polymer+Py-SO}_3^-)}$$

The Förster distance for the polystyrene–pyrene pair, corresponding to $E = 50\%$, is 19.4 Å as given by Berlman.[28] A similar procedure was also used to calculate E (=9%) according to the changes of the pyrene emission in the presence and absence of the copolymer. The accuracy of the latter procedure was not as good because of the slight scattering of the polymer solution.

When the pH of the solution was raised to 3.5, energy transfer between the styrene and Py-SO_3^- chromophores was absent as indicated by the unchanged styrene emission shown in Figure 13. This is clearly attributed to phase separation between the aggregated styrene domain and the imidazole domain. To further confirm such styrene aggregation, a pure pyrene at a concentration of 4×10^{-7} M in place of the Py-SO_3^- probe was introduced to the copolymer aqueous dispersion. Because of its preferential partitioning in the hydrophobic domain, energy transfer between pyrene and styrene was observed. The transfer efficiency of the latter pair of $E = 12.7\%$ was estimated

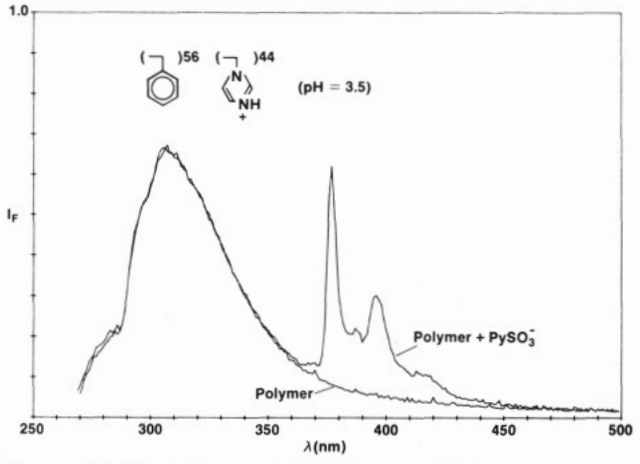

Figure 13. Emission spectra of StIm-56 ([St] = 0.005 M) in aqueous acetic acid (pH 3.5) in the absence and presence of the acceptor Py-SO_3^- (4×10^{-7} M).

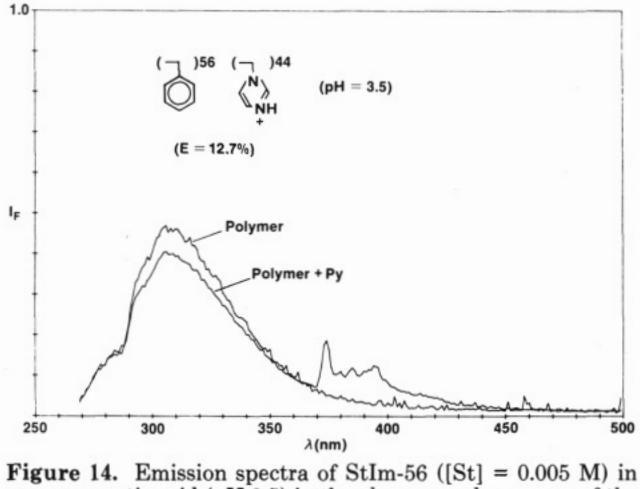

Figure 14. Emission spectra of StIm-56 ([St] = 0.005 M) in aqueous acetic acid (pH 3.5) in the absence and presence of the acceptor pyrene.

from the styrene emission spectra as shown in Figure 14 for StIm-56 in pH 3.5 acetic solution.

Phase separation of these random copolymers in aqueous dispersion, by fluorescence intensity measurements as a function of pH as discussed in a previous section, is thus further confirmed by energy-transfer studies. Manifestation of such phase separation can be achieved on solid film samples cast on water from a good organic solvent. The TEM of a film sample of StIm-30 is shown in Figure 15. The phase structure with domain size around 500–1000 Å is attributed to the reorientation of the hydrophobic styrene and the hydrophilic imidazole groups upon contact with the water surface. The domain separation in the film sample is more pronounced than that in the aqueous dispersion. Thermal measurements of the phase-separated film sample failed to yield two separate glass transitions, however, because of the annealing process taking place during the thermal measurement.

Conclusion

Phase separation of random copolymers of styrene and vinylimidazole can be observed by a variety of microscopic and macroscopic techniques. The smaller hydrodynamic volumes of the copolymers compared with those of the PVI homopolymer in polar media are a result of styrene aggregation. A conformational change of these copolymers from an acid-soluble extended coil to an intramolecular compact coil or intermolecular aggregate can be induced by pH increase. The styrene excimer formation in these

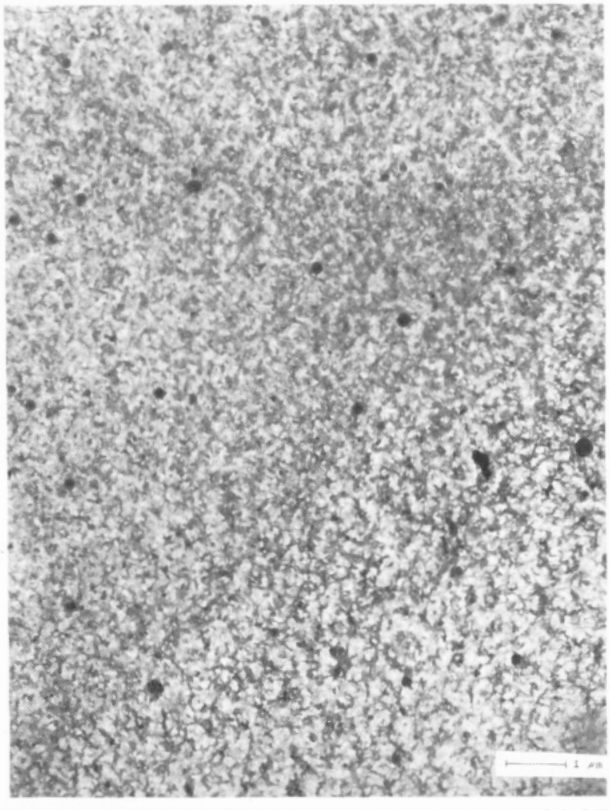

Figure 15. TEM of StIm-30 film cast on water from a MeOEt solution.

random copolymers is affected by the copolymer composition as well as long-range forces. While nearest-neighbor pairing of the phenyl rings is a prerequisite for excimer formation, it is enhanced by the long-range intrachain and interchain interactions. Phase separation between the styrene and the imidazole domains in aqueous dispersion was confirmed by energy transfer. Such domain separation is manifested in films cast on water, resulting from reorientation of the styrene and imidazole segments.

Acknowledgment. We are grateful to Drs. L. Schwartz and P. M. Henrichs for the use of their ^{13}C analysis procedure. We also appreciate the discussion and measurements of the glass transition temperatures provided by A. Marshall.

Registry No. (St)(Im) (copolymer), 60755-40-0.

References and Notes

(1) Ponticello, I. S.; Sutton, R. C.; Handel, T. M.; Bruemmer, T. M.; Martic, P.; Tan, J. S., to be submitted for publication.
(2) Edelman, G. M.; McClure, W. O. *Acc. Chem. Res.* **1968**, *1*, 65.
(3) Stork, W. H.; deHasseth, P. L.; Schippers, W. B.; Kormeling, C. M.; Mandel, M. *J. Phys. Chem.* **1973**, *77*, 1772.
(4) Tan, J. S.; Schneider, R. L. *J. Phys. Chem.* **1975**, *79*, 1380.
(5) Chen, T.; Thomas, J. K. *J. Polym. Sci., Polym. Chem. Ed.* **1979**, *17*, 1103.
(6) Tan, J. S.; Sochor, A. R. *Macromolecules* **1981**, *14*, 1700.
(7) Klein, G. W.; Snow, R. A.; Sutton, R. C. U.S. Patent 4 450 224, 1984.
(8) Petrak, K. L. *J. Polym. Sci., Polym. Lett. Ed.* **1978**, *16*, 393.
(9) Handel, T. M.; Ponticello, I. S.; Tan, J. S. *Macromolecules* **1987**, *20*, 264.
(10) Henrichs, P. M.; Whitlock, L. R.; Sochor, A. R.; Tan, J. S. *Macromolecules* **1980**, *13*, 1375.
(11) Whitlock, L. R., Kodak Research Laboratories, Eastman Kodak Co., unpublished data.
(12) Schwartz, L. J.; Henrichs, P. M., unpublished data for ^{13}C NMR analysis of similar copolymers.
(13) Miller, M. L. *The Structure of Polymers*; Reinhold: New York, 1966; Chapter 9.
(14) Vela, M.; Haebig, J.; Rice, S. *J. Chem. Phys.* **1963**, *43*, 886.
(15) Gelles, R.; Frank, C. W. *Macromolecules* **1982**, *15*, 741, 747.

(16) Torkelson, J. M.; Lipsky, S.; Tirrell, M. *Macromolecules* **1981**, *14*, 1601.
(17) Torkelson, J. M.; Lipsky, S.; Tirrell, M.; Tirrell, D. A. *Macromolecules* **1983**, *16*, 326.
(18) Abuin, E.; Lissi, E.; Gargallo, L.; Radic, D. *Eur. Polym. J.* **1984**, *20*, 105.
(19) Lindsell, W. E.; Robertson, F. C.; Soutar, I. *Eur. Polym. J.* **1981**, *17*, 203.
(20) David, C.; Lempereur, M.; Geuskens, G. *Eur. Polym. J.* **1973**, *9*, 1315.
(21) Reid, R. F.; Soutar, I. *J. Polym. Sci., Polym. Phys. Ed.* **1978**, *16*, 231.
(22) Turro, N. J.; Okubo, T. *J. Phys. Chem.* **1982**, *86*, 1485.
(23) Ander, P.; Mahmoudhagh, M. K. *Macromolecules* **1982**, *15*, 214.
(24) Major, M. D.; Torkelson, J. M. *Macromolecules* **1986**, *19*, 2801.
(25) Frank, C. W.; Semerak, S. N. *Adv. Polym. Sci.* **1984**, *54*, 31.
(26) Oyama, H. T.; Tang, W. T.; Frank, C. W. *Macromolecules* **1987**, *20*, 474.
(27) Morishima, Y.f Kobayashi, T.; Nozakura, S.; Webber, S. E. *Macromolecules* **1987**, *20*, 807.
(28) Berlman, I. B. *Energy Transfer Parameters of Aromatic Compounds*; Academic: New York, 1973; p 114.

Formation of a High Melting Crystal in a Thermotropic Aromatic Copolyester

Y. G. Lin and H. H. Winter*

Department of Chemical Engineering, University of Massachusetts, Amherst, Massachusetts 01003. *Received September 28, 1987*

ABSTRACT: The formation of a high melting crystal during melt annealing is observed for a thermotropic liquid crystalline polymer (LCP), VECTRA A900 of Celanese Corp. When the polymer is heated to 290 °C, i.e. just above its nominal DSC melting temperature of about 280 °C, it melts rapidly, displaying a low complex modulus of about 10^3 Pa. However, during annealing at this same temperature, the nematic melt slowly crystallizes and undergoes a liquid/solid transition, as shown by a gradual increase in the complex modulus by 3 orders of magnitude in 200 min. For DSC and X-ray studies, a discrete set of samples were prepared with increasing time of annealing at 290 °C and subsequent cooling to room temperature. Wide-angle X-ray scattering patterns of these samples shows an additional reflection ring with d = 3.8 Å. In the DSC first heating scan, the annealed samples display two separated endothermic peaks. The first peak is about 280 °C; the second peak is 20–30 K above the annealing temperature. The unannealed samples have only the first peak. As the annealing time increases, the first peak decays and the second peak grows and moves from 305 to 315 °C. The growth of the complex modulus is found to be proportional to the area under the second endothermic peak. All these observations indicate a gradual formation of a high melting crystal with a higher degree of order. The formation of the high melting crystal is thermoreversible. After being heated to a temperature above the DSC second endothermic peak, the annealed samples return to their initial state before annealing, displaying once again low complex modulus and a single endothermic peak. The rate of the crystallization depends on annealing temperature and on mechanical and thermal histories of the samples. Higher annealing temperature leads to slower crystallization. At 290 °C, stretched samples exhibit accelerated crystallization. It is interesting to note that samples which have been subjected to a prior heating to 320 °C do not show significant crystallization at 290 °C. This indicates that the crystallization is a nucleation and growth process and that the nuclei melt during the preheating to 320 °C.

Introduction

The crystallization behavior of liquid crystalline polymers (LCPs) has been the subject of several recent publications.[1-6] It is well-known that for flexible polymers the crystallization process can be quite rapid[7,8] because the flexible molecular chains can readily adjust their sequences into a growing crystalline structure. However, it is much more difficult for the rigid molecular chains of LCPs to diffuse appropriate sequences into a crystal growing location.[1] In the nematic melt state, rigid molecular chains arrange into a polydomain texture with high local order and long-range random orientation.[9-16] The local order determines the crystallization process. The crystals have little long-range order.[1] A matter worthy of note is that thermal and mechanical treatments can alter the local order[5,6,12-15] and hence can change the ability of crystallization of LCPs. These characteristics of LCPs complicate the phase behavior and the rheology in a wide temperature range.

Severe time dependence of rheological properties in the nematic melt state has been recently reported for copolymers of 73 mol % 4-hydroxybenzoic acid and 27 mol % 6-hydroxy-2-naphthoic acid in capillary flow[3] and for a quaterpolymer of chalorhydroquinone, 4,4′-dihydroxydiphenyl, terephthalic acid, and resorcinol in a mole ratio of 40/10/35/15 in dynamic mechanical measurements.[2] In both cases, DSC curves of the annealed samples showed a second endothermic peak at a temperature above the annealing temperatures. It is expected that these changes of rheology resulted from formation of some high melting crystalline structure.

Recently, a commercial liquid crystalline aromatic polyester (VECTRA A900, Celanese Corp.) has been extensively studied in our laboratory.[5,6] When this polymer is kept under isothermal conditions slightly above the melting temperature, its rheological stability depends strongly on prior thermal treatment. After preheating to 320 °C, the polymer melt shows relatively stable rheological properties throughout several hours.[6] However, if the sample is just melted and kept at 290 °C, without prior heating to an elevated temperature, the polymer melt displays a severe increase in the complex modulus. In the present work, these experimental observations are related to a gradual formation of a high melting crystal.

Experimental Section

The liquid crystalline polymer studied, VECTRA A900 (Celanese Corp.), is a random copolymer containing 73 mol % 4-hydroxybenzoic acid (HBA) and 27 mol % 6-hydroxy-2-naphthoic

0024-9297/88/2221-2439$01.50/0